PHYSICAL REVIEW B VOLUME 36, NUMBER 12 15 OCTOBER 1987-II

Effects of cation vacancies and diffusion on the surface states of $Hg_{1-x}Cd_xTe$

Garnett W. Bryant
McDonnell Douglas Research Laboratories, P.O. Box 516, St. Louis, Missouri 63166

(Received 2 February 1987)

The effects of cation vacancies and of cation diffusion on the surface states of otherwise ideal (100) cation- and anion-terminated surfaces of $Hg_{1-x}Cd_xTe$ have been investigated by use of the site-dependent coherent-potential approximation (SDCPA) for the alloy. Cation diffusion has been examined by use of model layer-dependent Hg and Cd concentrations. The effects of cation vacancies have been investigated by treating the cation vacancy, which has been modeled as an ideal point defect having orbitals with very large energies, on an equal footing with Cd and Hg when calculating the CPA cation self-energy. Bulk-vacancy levels occur near the valence-band edge. The defect levels are lower in energy when the vacancies are close to the surface. $Hg_{1-x}Cd_xTe$ (100) surface states that are sensitive to the alloy disorder have the character of the constituents, HgTe and CdTe, rather than that of some average effective constituent. The bimodal character of the surface density of states remains when surface vacancies are present or variations in composition occur. Results are presented for the bulk and surface densities of states and for the CPA self-energies to illustrate the sensitivity of the alloy surface states to cation vacancies and diffusion.

I. INTRODUCTION

Relativistic effects, which are present in Hg but weak in Cd,[1–3] lower the Hg 6s level so much relative to the Te 5p state that HgTe has an inverted band structure with a zero band gap and valence- and conduction-band-edge states derived from the anion p states. In contrast, CdTe has the normal semiconductor level ordering with anion-derived, valence-band-edge states and cation-derived, conduction-band-edge states. The large difference between the atomic-level orderings of HgTe and of CdTe has important consequences for the electronic structure of the bulk and surface states in $Hg_{1-x}Cd_xTe$. One consequence is that the electronic states of $Hg_{1-x}Cd_xTe$ alloys are more sensitive to alloy effects than are the states of other semiconductor alloys. States in $Hg_{1-x}Cd_xTe$ which are local in character and sensitive to the cation sites, such as the valence states 5 eV below the band edge[1,2] and the surface states of ideal (100) cation surfaces,[4,5] cannot be described by use of simple, effective-medium models for the alloy such as the virtual-crystal approximation (VCA). More sophisticated alloy models, such as the coherent-potential approximation (CPA), must be used to calculate accurate densities of states (DOS's). The localized states which are sensitive to the disorder have the character of the individual alloy constituents rather than of some average, VCA-like, constituent. For example, the ideal (100) cation surface has HgTe- and CdTe-like surface-state bands in the gap between the valence and conduction bands, but no virtual-crystal-related surface-state features in this energy range.[4,5]

A second consequence of the inverted level ordering of Hg 6s and Te 5p states is that the Hg—Te covalent bond is much weaker than the Cd—Te covalent bond.[1,3] In $Hg_{1-x}Cd_xTe$ alloys, Hg vacancies form easily and Hg diffuses readily.[6–8] In this paper the effects of Hg vacancies on the bulk and surface DOS's of $Hg_{1-x}Cd_xTe$ are calculated. We determine how the cation-vacancy levels shift when the vacancy is near a surface. We also determine how the alloy-induced bimodal character of the alloy surface states changes when the surface has cation vacancies. The effects of Hg diffusion, as manifested by variations in alloy composition x near a surface, on the surface DOS's are also determined. The results reflect the dependence of the surface DOS's on the bulk and surface composition.

Previously, we determined the surface states of ideal (100) cation and anion alloy surfaces.[4,5] The (100) surfaces were studied, in part, because the calculations are easier for (100) surfaces than for other surfaces and, in part, because alloy effects should be strongest (weakest) for (100) cation (anion) surfaces. In this paper we again consider (100) surfaces. In the previous studies the (100) surfaces were ideal, unrelaxed, and unreconstructed. While surface relaxation and reconstruction can greatly distort the electronic structure of an ideal surface, information presently available for $Hg_{1-x}Cd_xTe$ is not adequate to suggest a realistic choice for the surface structure. In this paper we again consider ideal surfaces. Until a reliable understanding of the surface structure of $Hg_{1-x}Cd_xTe$ is developed, our studies of ideal surfaces should provide a good qualitative measurement of the importance of alloy effects, vacancies,[9] and diffusion on alloy surface states.

In Sec. II a brief review of the model used to study $Hg_{1-x}Cd_xTe$ surface states is presented and the extension of the model to include vacancies and diffusion is described. The results are presented in Sec. III and conclusions are made in Sec. IV.

II. THEORY

The calculations are performed for (100) cation- and anion-terminated alloy surfaces. Tight-binding (TB) models are used to describe the alloy constituents. Extrapolation of these tight-binding models, fitted to reproduce bulk-band properties, to studies of localized states, especially in alloy systems where fluctuations in local environment are significant, must be done carefully. We use the second-nearest-neighbor TB Hamiltonians developed by Hass[2] to describe HgTe and CdTe. Spin-orbit effects are included by using a 16-state model with cation and anion s and p states for each spin. Hass chose the energy levels to be the atomic energies and determined the off-diagonal elements by fitting to experimental energy gaps and pseudopotential calculations. In Hass's model, the Te energy levels in HgTe and CdTe are chosen to be the same, as one would expect if charge-transfer effects are small. Other TB models[10–12] have also been developed for HgTe and CdTe by fitting predicted band structures to experimental energy gaps. However, Hass's model should describe localized states better than the other TB models in which the anion energy levels change as much between HgTe and CdTe as the cation levels change, even though the anion is the same. We generalized the Hass model by including couplings previously ignored[4,5] to obtain accurate conduction bands and masses. The tight-binding parameters are given in Refs. 2 and 5.

The alloy disorder effects are incorporated by use of effective-medium models. In this approach, the randomly occupied cation sites are occupied by effective atoms. In the VCA, the effective atom is defined by the compositionally weighted average of the HgTe and CdTe parameters. The VCA works well when the constituents are similar, and can even work well for dissimilar constituents like HgTe and CdTe if the states are well extended or insensitive to cation sites. Hass chose the anion diagonal terms to be identical for the two constituents and the off-diagonal terms of the two to be nearly the same. The VCA is assumed to be adequate for the alloy anion diagonal elements and the off-diagonal elements. The VCA bulk values for these matrix elements are used at all sites in all calculations reported here.

The cation diagonal elements must be modeled more carefully. The VCA can be used for these matrix elements to describe well-extended states but not localized states sensitive to the large difference between Hg and Cd s-state energy levels ($E_{s,\mathrm{Hg}}=-1.32$ eV, $E_{s,\mathrm{Cd}}=0.12$ eV). To provide a better model for the cation diagonal disorder, the coherent-potential approximation is utilized. The cation s-levels are described by self-energies for each spin and spin-mixing terms. The cation p levels are described with spin-independent self-energies. In the absence of vacancies, the self-energies are determined by requiring that the effective cation produce the same scattering as the composition-weighted average scattering of Hg and Cd embedded in the effective medium.[13,14]

All bulk, cation sites are equivalent so the same self-energy can be used for each bulk site. However, near a surface, translational symmetry is broken and the self-energy is site dependent. As a consequence, near a surface, a self-consistent self-energy must be found for each plane of equivalent sites. Model calculations[15–19] and realistic calculations[4,5] performed with the site-dependent coherent-potential approximation (SDCPA) confirm that the site dependence must be included to adequately model alloy effects on the surface states. Neither the VCA nor a site-independent CPA, in which the bulk self-energy is used for all sites, adequately models the alloy effects on all surface states.

To study the effects of cation diffusion near a surface, we assume that the Hg and Cd concentrations are constant in an atomic plane parallel to the surface but can vary from plane to plane. Furthermore, we assume that diffusion by one cation is compensated by diffusion of the other cation. Thus, if the Cd concentration in a particular plane is x, then the Hg concentration is $1-x$. We also assume that the alloy is random so that x is the same at all cation sites in the same plane. In effective-medium alloy models which use compositionally weighted averages, of the TB parameters in the VCA and the scattering in the SDCPA, diffusion is included by using a layer-dependent x in the averages. More complicated models for the cation diffusion which include intraplane diffusion could be considered. However, our calculations require that all cations in a plane be equivalent, so intraplane variations in x have not been included.

To treat vacancies within the CPA or VCA, we assume that the vacancy is another cation which must be included in the compositionally weighted averages. We assume that the vacancy concentration x_v is constant in a layer parallel to the surface but may vary from layer to layer. If the Cd concentration in a layer is x, then the Hg concentration is $1-x-x_v$.

In the TB formalism the ideal point vacancy is usually modeled[10,12] as an atom in an undistorted lattice with orbital energies that are chosen to be infinite so that the orbitals will be empty. We use this model but choose, in practice, finite energies for the s and p orbitals. Sufficiently large energies are used (1000 eV for s orbitals and 1200 eV for p orbitals) to ensure that the results are insensitive to the model. The results are sensitive when orbital energies of about 10 eV are used.

In the previous calculations of $\mathrm{Hg}_{1-x}\mathrm{Cd}_x\mathrm{Te}$ surface states,[4,5] thick films with more than 2000 layers were used to study bulk and surface states. Such films are wide enough to eliminate all surface-surface coupling but can still be treated efficiently by use of a renormalization-decimation (RD) approach.[4,5,17,20] We use the RD approach for the present calculations as well. In the previous SDCPA calculations, the site dependence of the self-energy was included for the two layers of cations closest to the surface. All other cation layers were modeled with the bulk self-energy. Similarly, in this paper x and x_v differ from the bulk values only for the two cation layers closest to the surface.

III. RESULTS

A. Bulk vacancies

Calculations[10–12] for the energy levels of isolated bulk cation vacancies in $\mathrm{Hg}_{1-x}\mathrm{Cd}_x\mathrm{Te}$ predict that the vacan-

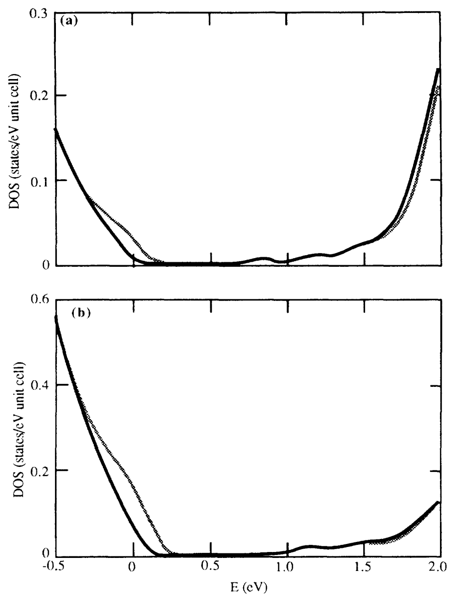

FIG. 1. Densities of states of $Hg_{1-x}Cd_xTe$ at bulk cation (a) and anion (b) sites when $x_v=0$ (solid curves) and $x_v=0.01$ (coded curves). In each case $x=0.5$.

cies are shallow acceptors with energy levels near the valence-band edge. Experimental results[6,7] support this prediction. Figure 1 shows the densities of states, near the fundamental band gap, at bulk cation and anion sites of $Hg_{1-x}Cd_xTe$ ($x=0.5$) with no cation vacancies ($x_v=0$) and with 1% cation vacancies ($x_v=0.01$). When vacancies are present, the DOS near the valence-band edge increases (see Fig. 2). Our results are consistent with the expectation that the cation vacancy is a

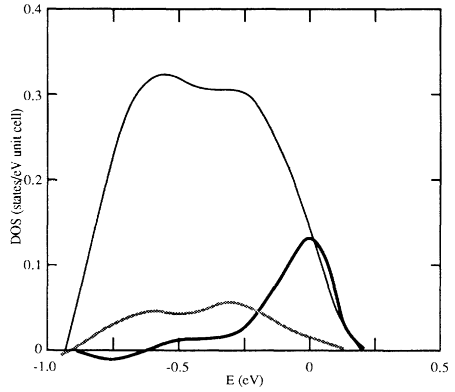

FIG. 2. The vacancy-induced change in the DOS near the valence-band edge: The change in the bulk, anion-site DOS when $x_v=0.01$ at all sites (thick solid curve); and the change in the DOS at an anion site next to a cation surface when $x_v=0.01$ at all sites (coded curve) and when $x_v=0.01$ at the bulk sites, 0.05 at cation sites next-nearest to the surface, and 0.1 at cation sites on the surface (thin solid curve). In all cases $x=0.5$.

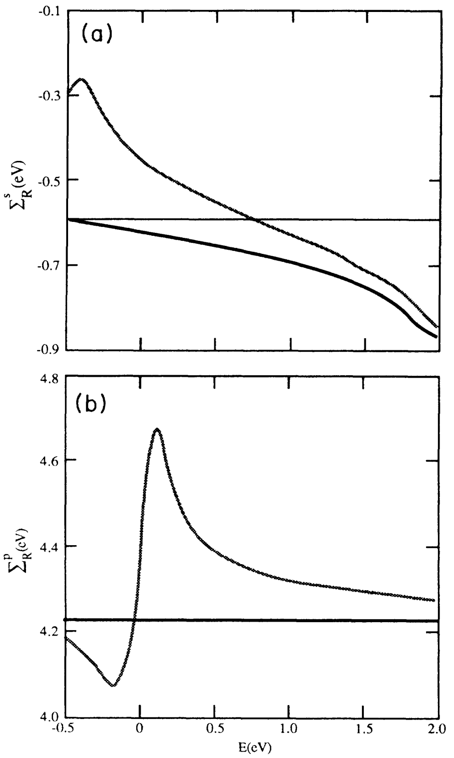

FIG. 3. Real parts of the bulk, diagonal, s, and p self-energies when $x_v=0.01$ (coded curves) and $x_v=0$ (solid curves). The solid, straight line in the top panel is the VCA cation s level. In all cases $x=0.5$.

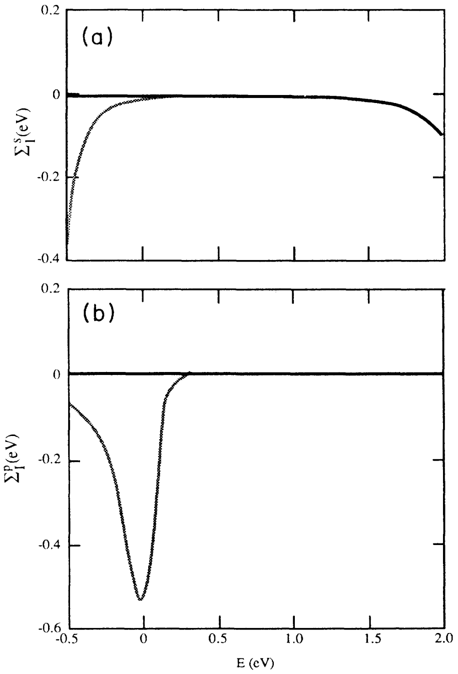

FIG. 4. Imaginary parts of the bulk, diagonal, s, and p self-energies when $x_v=0.01$ (coded curves) and $x_v=0$ (solid curves). In all cases $x=0.5$.

shallow acceptor. The increase near the band edge in the cation-site DOS is similar to the increase in the anion-site DOS, only reduced in scale by a factor of 5. Small, insignificant changes occur in the conduction-band DOS and in the valence-band DOS away from the band gap.

Figures 3 and 4 show the real and imaginary parts, respectively, of the bulk, diagonal, *s*, and *p* self-energies in $Hg_{1-x}Cd_xTe$ with and without vacancies. In $Hg_{1-x}Cd_xTe$ without vacancies, only the *s* self-energies differ from the VCA value. However, large changes occur in both the *s* and *p* self-energies near the valence-band edge when vacancies are present. Changes in the *s* self-energy also occur deep in the valence band and in the conduction band at energies for which the DOS is unchanged. While the structure in the *p* self-energy is correlated with the changes in the DOS due to vacancies, the significance of changes in the *s* self-energy is unclear since the changes can occur at energies for which the DOS is unchanged.

B. Surface vacancies

The effects of vacancies on the surface DOS's of $Hg_{1-x}Cd_xTe$ are shown in Figs. 2, 5, and 6 for (100) cation and anion surfaces. Two cases have been considered. In the first case, the vacancy concentration is the same ($x_v = 0.01$) at all cation sites. In the second case, $x_v = 0.10$ at the cation sites closest to the surface, $x_v = 0.05$ at the cation sites next nearest to the surface, and $x_v = 0.01$ at all other bulk cation sites. In each case the Cd concentration is $x = 0.5$ at all sites. Results for $Hg_{1-x}Cd_xTe$ without vacancies are shown for comparison.

The vacancy-induced increase in the DOS near the valence-band edge of an anion site next to a cation surface (Fig. 2) has two peaks which are deeper in the valence band than the peak in the vacancy-induced DOS of a bulk anion site. The peak at -0.6 eV (-0.3 eV) is identified with vacancies at cation sites on (next to) the cation surface. The increase in the peak at -0.6 eV is greater than the increase in the peak at -0.3 eV when the concentration of vacancies at the surface increases from 0.01 to 0.10, but the concentration at the site next to the surface increases only from 0.01 to 0.05. Unambiguous identification of defect states at vacancies near anion surfaces is difficult because the DOS for such states overlaps with the anion surface-state DOS.

The bimodal character of the (100) ideal-cation-surface DOS is apparent in Fig. 5. The band at lower energy in the main gap is HgTe-like, the upper band is CdTe-like. Cation vacancies near the surface have little effect on the surface-state DOS, especially when $x_v \sim 0.01$. The bands do broaden when vacancies are present. Also the bands, especially the HgTe band, shift to slightly higher energies because the band gap is wider when vacancies are present. Moreover, the bimodal character of the cation-surface-state DOS remains even when $x_v = 0.1$. The bimodal character is reflected in the peak heights. The ratio of HgTe to CdTe surface-state DOS peak heights decreases when Hg vacancies are present at the surface.

The dispersion of the cation surface states is not affected much by vacancy concentrations less than 10%. Inspection of the *k*-dependent DOS shows that surface states throughout the surface Brillouin zone shift by

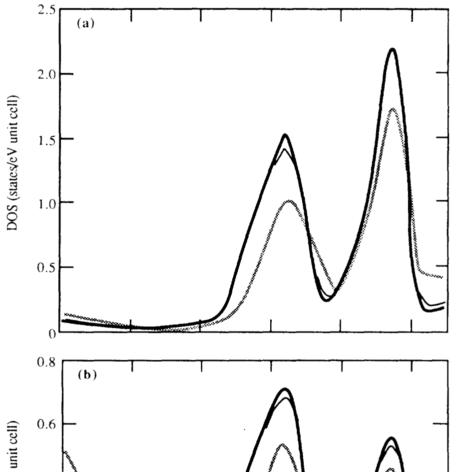

FIG. 5. Densities of states at cation (a) and anion (b) sites closest to a (100) cation surface of $Hg_{1-x}Cd_xTe$: with no vacancies (thick solid curves); $x_v = 0.01$ at all sites (thin solid curves); and $x_v = 0.01$ in the bulk, $x_v = 0.1$ at the cation surface site, and $x_v = 0.05$ at the next cation site in from the surface (coded curves). In all cases $x = 0.5$.

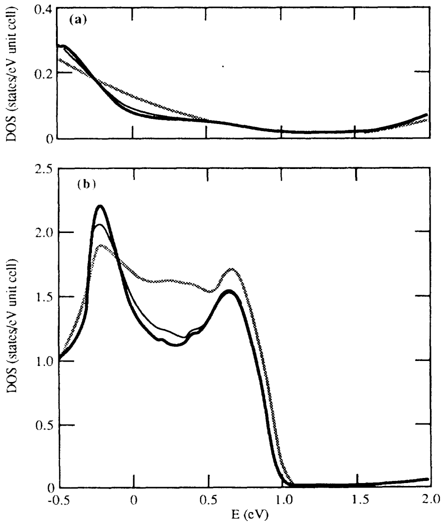

FIG. 6. Densities of states at cation (a) and anion (b) sites closest to a (100) anion surface of $Hg_{1-x}Cd_xTe$. The curves are labeled as in Fig. 5. In all cases $x = 0.5$.

similar amounts when the vacancies are present. However, some detail in the k-dependent DOS is broadened away when vacancies are present. For example, the spin-induced splitting of the surface states which is present in HgTe, CdTe, and the alloys,[4,5] disappears when $x_v = 0.10$. However, well-defined peaks in the surface DOS remain when vacancies are present which can be identified as the surface states.

The CPA calculations have included only diagonal-disorder effects. Off-diagonal disorder would provide additional broadening to the DOS. Off-diagonal–disorder effects were minimized for the pure alloy by use of similar off-diagonal matrix elements for the constituents. In a model for the vacancy with finite orbital energies, off-diagonal disorder could be more important. However, vacancy-included broadening from diagonal disorder does not qualitatively change the bimodal character of the surface states. We do not expect off-diagonal disorder to qualitatively change the bimodal character either, because the HgTe and CdTe surface states are separated by 1 eV.

The surface states of the anion surface (Fig. 6) are VCA-like in the alloy. When vacancies are present, the structures in the DOS are broadened and the vacancy levels near the valence-band edge overlap the anion surface states. The structure in the DOS of the anion site at an anion surface is distinguishable even when $x_v \sim 0.1$, but the weak structure in the DOS of the cation site next to an anion surface is not apparent when $x_v \sim 0.1$.

Vacancies induce changes in the self-energies at the cation sites closest to the cation and anion surfaces. The vacancy-induced changes in the self-energies at the cation site next to the anion surface account for the broadening of the anion surface states. Vacancy-induced changes in the s and p self-energies at the cation surface occur near the valence-band edge. However, in the energy region of the surface-state bands, the vacancy-induced changes in the cation surface self-energy are small. This insensitivity of the surface-state self-energies to vacancies reconfirms the bimodal, local character of the surface-state bands. Since no vacancy states exist at the cation surface at energies in the surface-state bands, the surface states are only HgTe- and CdTe-like.

C. Cation diffusion

Calculations have been performed for Hg-rich and Hg-depleted surfaces. In the case of a Hg-rich surface, the surface cation layer has a Cd concentration $x = 0.3$, in the next cation layer $x = 0.4$, and in all other layers $x = 0.5$. In the case of a Hg-depleted surface, the Cd concentrations are 0.5 at the surface, 0.4 at the next cation layer, and 0.3 in the bulk. In Figs. 7–9 we present results for the Hg-rich surface. Results for the Hg-depleted surface are similar.

The DOS at the cation and anion sites closest to the cation surface of the alloy with the Hg-rich surface are shown in Figs. 7 and 8 and compared with the surface DOS's of alloys with no diffusion ($x = 0.3$ and $x = 0.5$). Near the valence-band edge, the differences between the three DOS's are not great. However, the valence-band DOS at the Hg-rich surface is closest to the DOS of the uniform alloy that has the same bulk concentration ($x = 0.5$).

Two effects determine the surface-state DOS of the Hg-rich surface. The peak heights and shapes (for example, the shoulder in the HgTe-band) of the DOS of the Hg-rich surface are comparable to the peak heights and shapes of the DOS of the uniform alloy which has the same composition, $x = 0.3$, at all sites as the composition of the Hg-rich surface. However, the peak positions of the surface DOS for a Hg-rich surface are comparable to the peak positions for the uniform alloy

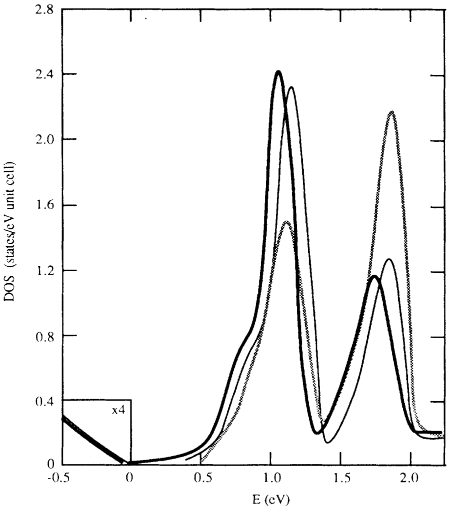

FIG. 7. Densities of states at a cation site on a (100) cation surface of $Hg_{1-x}Cd_xTe$: a uniform alloy, $x = 0.3$ (thick solid curve); a uniform alloy, $x = 0.5$ (coded curve); and an alloy with a Hg-rich surface, $x = 0.3$ at cation sites on the surface, $x = 0.4$ at cation sites next-nearest to the surface, and $x = 0.5$ at all other sites (thin solid curves). The results for the last two cases are nearly identical in the valence band so the coded curve is not shown.

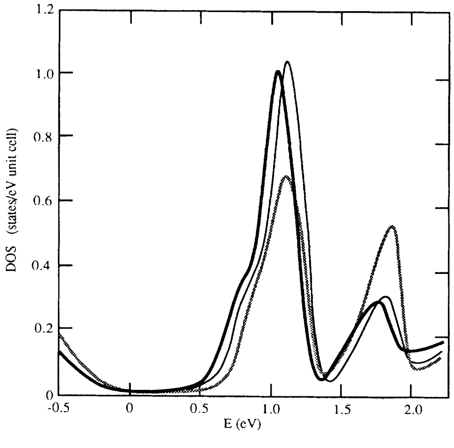

FIG. 8. Densities of states at an anion site closest to a (100) cation surface of $Hg_{1-x}Cd_xTe$. The curves are labeled as in Fig. 7. The coded and light solid curves coincide in the valence band.

which has the same composition, $x=0.5$, at all sites as the bulk composition of the alloy with an Hg-rich surface. The peak heights and shapes are determined by the surface composition while the positions are determined by the bulk composition. These relationships also hold when the surface is Hg depleted.

The s self-energies at the Hg-rich cation surface and at the cation surfaces of the uniform alloys are shown in Fig. 9. The structure in the surface s self-energy for uniform alloys is located so that (1) the real part of the s self-energy is approximately that of the s-level energy of the dominant cation at the energies of the surface-state band of the dominant cation and (2) so that variations in the self-energy occur in the region of the other surface-state band.[5] As a consequence, the structure in the self-energy of a uniform alloy shifts to lower energies as x increases. The structure in the s self-energy of the Hg-rich surface occurs at higher energy than the structure in the surface self-energy of either uniform alloy.

Although the surface states of the Hg-rich surface occur at the energies expected for the surface states of the uniform alloy with the same bulk composition, the Hg-rich surface does not behave like the surface of the uniform, $x=0.5$, alloy. The peak heights and shape are correlated to surface composition and the structure of surface self-energy of the Hg-rich surface is at higher rather than lower energies than the structure in the surface self-energy of the uniform, $x=0.3$, alloy. Surface-state energies are located in bulk-band gaps because the states decay into the bulk. Also, the cation surface-states are cation derived. Thus the surface states of the Hg-rich surface are tied to the bulk ($x=0.5$) conduction-band edge even though the surface behaves more like the surface of a uniform, $x=0.3$, alloy.

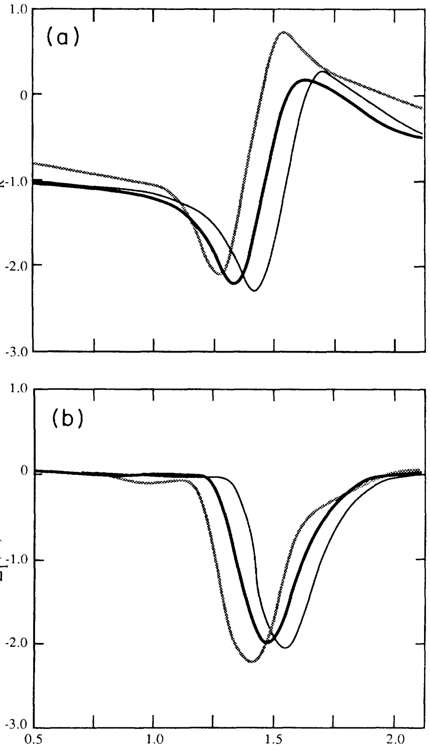

FIG. 9. The real and imaginary parts of the s self-energy for a cation at the (100) cation surface. The curves are labeled as Fig. 7.

The surface states of the anion surface of uniform $Hg_{1-x}Cd_xTe$ are VCA-like, with no bimodal character. In fact, VCA and CPA calculations yield almost identical results.[5] In alloys with diffusion, the anion surface-state DOS is almost identical to the surface-state DOS of the uniform alloy with the same bulk composition. The positions of the structure in the surface DOS are the same because the positions are determined by bulk-band structure. Moreover, the peak heights are the same, because the states have no bimodal character and thus are not sensitive to the surface composition. However, the self-energy of the cation site closest to the anion surface is sensitive to the surface composition. The self-energy at that site in the alloy with diffusion is nearly identical to the self-energy at that site in the uniform alloy with the same surface composition.

In performing the calculations, we used the bulk VCA values for anion matrix elements and off-diagonal matrix elements at all sites. While this may not be the most accurate modeling of these matrix elements when diffusion is present, it is the simplest modeling to implement. Off-diagonal matrix elements and anion matrix elements should influence the dispersion of the surface states. Since the bandwidths of the surface-state bands of the uniform, $x=0.3$ and $x=0.5$, alloys are similar, we do not expect the results to be sensitive to how these matrix elements are modeled when there is diffusion.

IV. CONCLUSION

The structure in the surface-state DOS of $Hg_{1-x}Cd_xTe$ without vacancies reflects the bimodal character, either HgTe-like or CdTe-like, of the cation surface states. We have studied surfaces with up to 10% cation vacancies. The vacancies do broaden and shift the surface-state DOS. However, the distinct bimodal character of the alloy cation-surface-state DOS is preserved. Local perturbations such as vacancies do not significantly distort the surface states because the surface states are also local in character. Large concentrations ($x_v > 0.1$) of vacancies would be needed to distort the surface states. The dispersion of the (100)-surface states does not change dramatically when vacancies are present. This is consistent with the finding[8] for (110) surfaces that the dispersion is insensitive to vacancy concentrations of less than 10%. The vacancies do induce additional states near the valence-band edge. States trapped at vacancies closest to the cation surface have the lowest energies. States trapped at vacancies near anion surfaces overlap anion-surface-state bands and are difficult to identify.

We have studied ideal, cation vacancies. In principle, lattice relaxation around the vacancy should be included. However, the presence of ideal vacancies at the surface does not significantly distort the surface states or their bimodal character. We would not expect the extra perturbation of vacancy lattice relaxation to qualitatively distort the surface states. Vacancy lattice relaxation would, however, shift the energies of the vacancy levels just as moving the vacancy from the bulk to the surface shifts the vacancy levels.

Calculations for other surfaces, such as the (110) surface, should be done. Cation (100) surface states are local in character and insensitive to surface vacancies. Surface vacancies might have more effect on other surfaces which have surface states with different character.

The surface DOS of Hg-rich and Hg-depleted surfaces depend on both the bulk, x_b, and surface, x_s, cation concentrations. When x_s is different from x_b, the number of states in the HgTe and CdTe surface-state bands is correlated with x_s. However, the positions of the bands are correlated with x_b. Since the states decay in the bulk region, the bulk-band gap rather than the surface-band gap determines the forbidden energy regime in which surface states can exist. Concentration variations which are larger than those we have studied or which extended deeper into the bulk would be needed to substantially modify the surface states.

Only ideal (100) alloy surfaces have been considered because adequate information for the alloy surface relaxation and reconstruction is not available. Surface relaxation or reconstruction can significantly change ideal-surface states. However, inclusion of surface relaxation and reconstruction should not change the qualitative effects of surface vacancies because the surface vacancies do not significantly distort the surface states. The interplay between surface relaxation effects and diffusion effects could be more complex. When diffusion occurs, the surface-state energies are correlated with x_b. However, surface relaxation and the shifts of surface state energies induced by the relaxation should be more strongly correlated to x_s because significant surface relaxations would occur only in the layers closest to the surface.

ACKNOWLEDGMENT

This work was performed under the McDonnell Douglas Corporation Independent Research and Development program.

---

[1] W. E. Spicer, J. A. Silberman, J. Morgen, I. Lindau, J. A. Wilson, A.-B. Chen, and A. Sher, Phys. Rev. Lett. **49**, 948 (1982).

[2] K. C. Hass, H. Ehrenreich, and B. Velický, Phys. Rev. B **27**, 1088 (1983).

[3] M. Janos and P. S. Guimarães, J. Phys. C **18**, L117 (1985).

[4] G. W. Bryant, Phys. Rev. Lett. **55**, 1786 (1985).

[5] G. W. Bryant, Phys. Rev. B **35**, 5547 (1987).

[6] W. E. Spicer, J. A. Silberman, I. Lindau, A.-B. Chen, A. Sher, and J. A. Wilson, J. Vac. Sci. Technol. A **1**, 1735 (1983).

[7] C. E. Jones, K. James, J. Mertz, R. Braunstein, M. Burd, M. Eetemadi, S. Hutton, and J. Drumheller, J. Vac. Sci. Technol. A **3**, 131 (1985).

[8] C. K. Shih, D. J. Friedman, K. A. Bertness, I. Lindau, W. E. Spicer, and J. A. Wilson, J. Vac. Sci. Technol. A **4**, 1997 (1986).

[9] Shih (Ref. 8) found that the structure of a (110) surface does not change when Hg vacancies are created near the surface. At present we have no reason to expect that surface vacancies modify the (100) surfaces either.

[10] C. A. Swarts, M. S. Daw, and T. C. McGill, J. Vac. Sci. Technol. **21**, 198 (1982).

[11] A. Kobayashi, O. F. Sankey, and J. D. Dow, Phys. Rev. B **25**, 6367 (1982).

[12] C. Tuncay and M. Tomak, Solid State Commun. **50**, 1065 (1984).

[13] P. Soven, Phys. Rev. **156**, 809 (1967).

[14] R. J. Elliott, J. A. Krumhansl, and P. L. Leath, Rev. Mod. Phys. **46**, 465 (1974).

[15] N. F. Berk, Surf. Sci. **48**, 289 (1975).

[16] G. W. Bryant, Surf. Sci. **154**, 435 (1985).

[17] G. W. Bryant, Phys. Rev. B **31**, 5166 (1985).

[18] H. Ueba and S. Ichimura, Phys. Status Solidi B **92**, 307 (1979).

[19] A. Zagorski and W. Nazarewicz, Acta Phys. Pol. A **57**, 403 (1980).

[20] M. P. López Sancho, J. M. López Sancho, and J. Rubio, J. Phys. F **25**, 851 (1985).